ELSEVIER

Journal of Nuclear Materials 282 (2000) 245–254

journal of nuclear materials

www.elsevier.nl/locate/jnucmat

Thermally induced gallium removal from plutonium dioxide for MOX fuel production

D.G. Kolman *, M.E. Griego, C.A. James, D.P. Butt [1]

Materials Corrosion and Environmental Effects Laboratory, Nuclear Materials Technology Division, Los Alamos National Laboratory, MS-E530, P.O. Box 1663, Los Alamos, NM 87545, USA

Received 1 May 2000; accepted 17 July 2000

Abstract

A dry process for separating Ga_2O_3 from PuO_2 – 1 wt% Ga_2O_3 powder was developed. PuO_2–Ga_2O_3 powder was exposed to flowing Ar–6% H_2 at 600–1200°C. Under these conditions, Ga_2O_3 is reduced to Ga_2O, a volatile species. Ga_2O, which is stable in a reducing environment at temperatures greater than 800°C, evolves and is collected downstream. Different process parameters were varied in an effort to optimize thermally induced gallium removal (TIGR). Exposure temperature had the greatest effect on TIGR. Temperatures of at least 1000°C were required to obtain discernible TIGR. As little as 25 wppm Ga remained after processing PuO_2 at 1200°C. It is likely that a further reduction in retained Ga can be attained by increasing the processing temperature. Ga removal was shown to increase with process time. However, the benefit in processing beyond 4 h is limited for this system. The lack of effect of sample volume and gas flow rate on TIGR suggests that Ga removal is limited by mass transport within the powder particles. The fact that Ga removal is less efficient in more coarse PuO_2 powders supports this hypothesis.

1. Introduction

Recent arms control initiatives dictate that the United States convert the plutonium metal from weapons into a form that cannot readily be returned to metal and that may be inspected by international organizations. In January 1997, the Secretary of Energy of the United States signed a Record of Decision finalizing a dual-track strategy to irreversibly dispose of the nation's surplus plutonium. The strategy allows for immobilizing plutonium in inert forms or burning plutonium as mixed oxide (MOX) fuel in existing reactors. There is one potential drawback in using weapons grade plutonium as feed for MOX fuel – weapons grade plutonium contains approximately 1 wt% gallium. Gallium is known to degrade the properties of many metallic materials via corrosion, embrittlement, or intermetallic compound formation [1–17]. Thus, there is significant concern that gallium present in MOX fuel will compromise zirconium-based fuel cladding [16,18]. A second concern is the detrimental effect of 1 wt% Ga on MOX fuel performance and processibility. The level of Ga that can be tolerated in MOX fuel is not known, but levels of 10 ppm in the MOX fuel (approximately 200 ppm in PuO_2 before blending) appear acceptable based on various studies [16,18,19].

PuO_2–Ga_2O_3 particles, which originate from oxidized Pu–Ga alloys, are composed of PuO_2 grains having limited Ga_2O_3 solubility plus second-phase Ga_2O_3 grains having limited PuO_2 solubility. Thus, the powder materials are not simple mixtures which can be mechanically separated. Methods for chemically purifying plutonium metal have long been established [20]. These methods use aqueous solutions to dissolve and concentrate the material. Unfortunately, these methods can produce significant mixed waste (i.e., waste containing both radioactive and chemical hazards). The treatment and disposal of the large volume of waste resulting from

* Corresponding author.

[1] Present address: Department of Materials Science and Engineering, Rhines Hall, P.O. Box 116400, University of Florida Gainesville, FL 32611-6400, USA.

0022-3115/00/$ - see front matter
PII: S0022-3115(00)00397-4

aqueous purification of tens of metric tons would be expensive. A new, 'dry' method of purification is required.

Ga_2O, a species that is unstable at room temperature, can be stable in the gas phase at elevated temperatures [21,22]. It was hypothesized that Ga_2O_3 could be separated from PuO_2 by passing a reducing gas, H_2, over the PuO_2–Ga_2O_3 powder to produce Ga_2O via the reaction

$$Ga_2O_{3(s)} + 2H_{2(g)} \rightarrow Ga_2O_{(g)} + 2H_2O_{(g)}. \quad (1)$$

Preliminary experiments indicated that Ga_2O could indeed be vaporized from Ga_2O_3 in flowing H_2 gas and transported downstream [22]. However, it was unclear whether Ga_2O could be vaporized from PuO_2 incorporating Ga_2O_3. It is the objective of this work to examine the viability of thermally induced gallium removal (TIGR) from PuO_2 using a reducing gas. A second goal of this work is to determine the factors affecting gallium removal in an effort to optimize the TIGR process.

2. Experimental procedure

2.1. Material characteristics

Two types of PuO_2–Ga_2O_3 were used for this study. The first was a relatively fine powder produced from Pu–Ga metal using a three-step process, wherein the metal is hydrided, the hydride is nitrided, and the nitride is oxidized [23]. Scattered light analysis of the powder indicated a bimodal particle size distribution with a significant fraction of the powder comprising submicron particles (Fig. 1, Lab-Tec particle size analyzer). An electron micrograph of the three-step powder is shown in Fig. 2. Chemical analysis of this powder indicated a Ga concentration of 0.84 wt% (8400 μg/g (wppm)) or 1.1 at.%. The second type of PuO_2 (Ga concentration = 8000 wppm) was produced using a direct metal oxidation (DMO) method wherein the metal is converted directly to oxide in air at approximately 600°C. As compared to the three-step process, the DMO method produces a more coarse powder (Fig. 1) having less surface area per gram (Table 1, Quantachrome NOVA-1000 BET surface area analyzer). Loss-on-ignition (LOI) was used to estimate the quantity of water adsorbed on the powder surface. LOI is determined by heating a powder sample to 1000°C for 2 h in air and measuring mass loss [24]. For the three-step and DMO powders, LOI was 0.58% and 0.073%, respectively. Particle size, surface area, and LOI data represent the average of two measurements (measurement errors (S.D.) of 5.8%, 12% and 33%, respectively). The chemical compositions of the powders, determined by a variety of standard analysis techniques (primarily inductively coupled plasma-mass spectroscopy (VG Elemental Plasma Quad 2) and inductively coupled plasma-atomic emission spectroscopy (Thermo Jarrell Ash IRIS CID)), are shown in Table 2. These values are the average of four to seven separate measurements. Commercially pure Ga_2O_3 powder (Alfa Aesar) had a reported purity of 99.999% (metal basis).

2.2. Test Procedure

TIGR tests comprised the exposure of PuO_2–Ga_2O_3 to high-purity Ar–6% H_2 gas ($O_2 < 8$ ppm, $H_2O < 0.7$

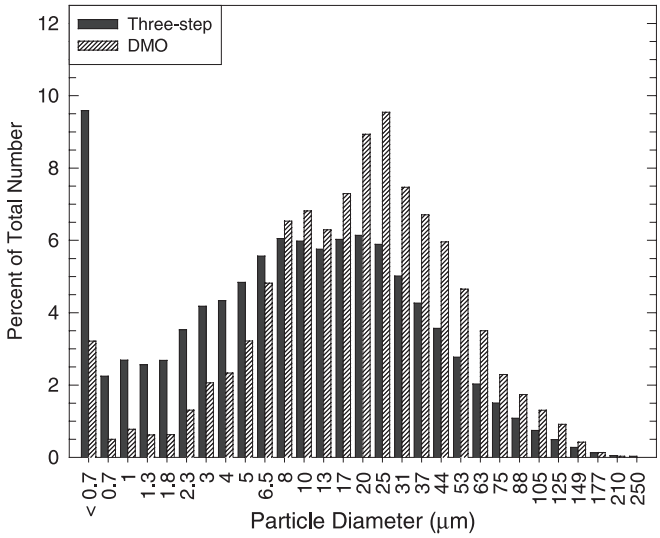

Fig. 1. Particle size distributions of the PuO_2 powders used in this study.

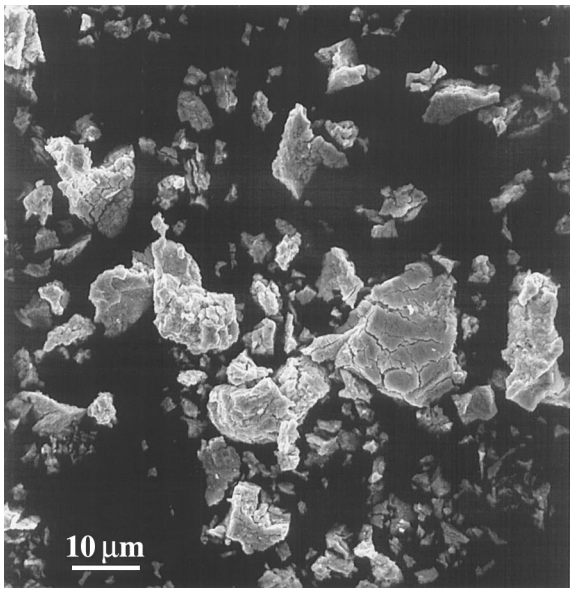

Fig. 2. Micrograph of three-step PuO_2 powder.

Table 1
Specific surface areas of various powders

	Three-step	DMO
Untreated	6.7 $m^2/g \pm 0.3$	1.7 $m^2/g \pm 0.2$
Following TIGR (1200°C; 4 h; 1.5 cm/s)	0.21 m^2/g	

ppm). Tests were performed within the confines of an Ar-atmosphere glove box. For the majority of small sample tests (typically 0.3, 0.9 and 2.5 g), three samples were simultaneously exposed (see Fig. 3). Simultaneous exposure of three samples yielded results identical to individual exposures. Each PuO_2 sample was weighed, placed in a nonreactive alumina boat, and then weighed again, noting the total mass of the boat and its contents. These small boats were then placed in a single large alumina boat to facilitate handling. Samples larger than 2.5 g were placed directly in a large boat and exposed individually. The large boat was inserted into the hot zone of a 4.45 cm (1.75 in.) I.D. tube furnace. The hot zone temperature was uniform. The temperature was ramped at a rate of 20°C/min until the temperature of interest was reached. The samples were held at this temperature for a fixed period of time. At the end of this period, the furnace was turned off and the samples were allowed to cool while maintaining gas flow. Reported test durations include only time at temperature and do not incorporate ramp time. Following cooling to nearly room temperature (<50°C), the samples were removed from the furnace and the gross mass of the boats recorded. Temperature, exposure duration, sample mass, and gas flow velocity were varied in an effort to determine the rate limiting step and thus optimize Ga removal. Two to four replicate tests were performed for most combinations of time, temperature, flow velocity and sample size. A total of 270 experiments were performed. Reproducibility was ±8% for mass loss values and ±50% for Ga concentration values based on statistical analyses of experiments that incorporated four replicate tests.

3. Results

3.1. Effect of temperature

The remaining Ga concentration in three-step PuO_2 powder following exposure to Ar–6% H_2 at different temperatures is shown in Fig. 4. 0.5 h exposures at 600°C and 800°C resulted in essentially no measurable Ga removal, and 900°C exposures yielded only slight Ga removal. Fig. 4 indicates that a temperature of at least 1000°C is required to obtain significant Ga removal. At 1200°C, the Ga concentration was reduced to approximately 150 ppm for a 0.5 h exposure.

Processing at 1200°C resulted in coarsening of the powders, as determined by scattered light particle size analysis (Figs. 5 and 6). Processing also resulted in a dramatic reduction in surface area (Table 1).

3.2. Effect of time

The effect of test duration on TIGR is shown in Fig. 7. Increasing exposure time reduces the concentration of Ga remaining in the samples. For the 24 h exposure (Fig. 7), the Ga concentration is reduced by greater than two orders of magnitude (from 8400 to 33 ppm). However, increasing test duration yields

Table 2
Primary impurity concentrations in three-step and DMO powders. Values are μg/g of PuO_2. Standard deviations are given as percent of average values

	Ga	H	N	C	Fe	U	Ca	Si	Ni	Cl	Cr	F	Zr	Al	Cu	S
Three-step	8400	510	360	330	240	160	89	79	91	75	48	45	36	27	25	8
DMO	8000	180	320	130	360	98	130	83	95	110	110	34	17	20	24	6
S.D. (%)	7.3	9.2	11	55	34	6.8	41	11	31	68	23	57	21	48	20	59

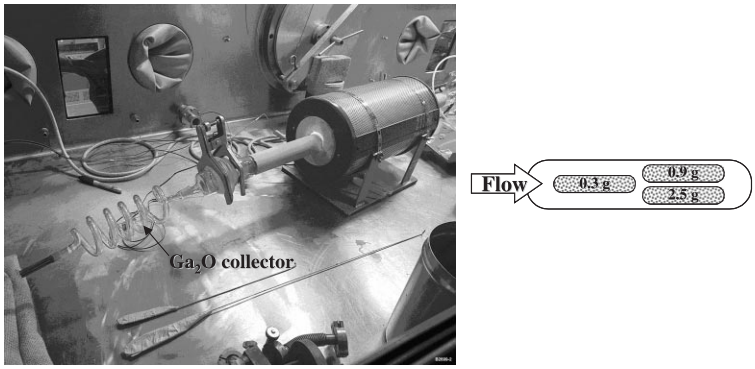

Fig. 3. Picture of furnace setup (left), drawing of boat placement within furnace (top right), and arrangement of small boats within the large boat (bottom right).

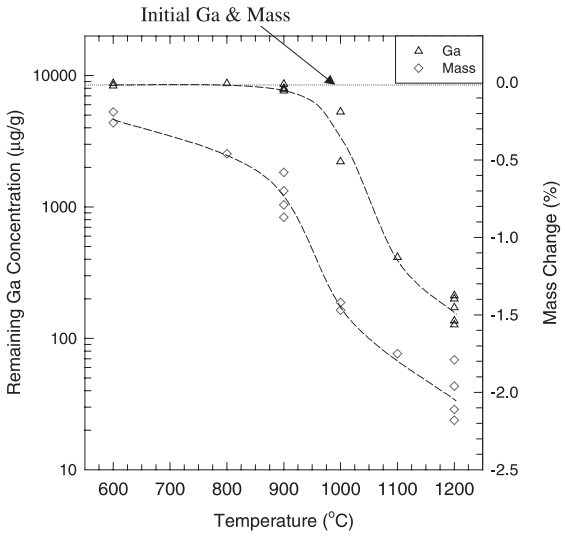

Fig. 4. Remaining Ga concentration in, and mass loss from, three-step powder as a function of exposure temperature in flowing Ar–6% H_2. Test duration: 0.5 h; sample mass: 2.5 g; flow velocity: 1.5 cm/s.

diminishing returns with respect to Ga removal. For instance, the majority of the Ga is removed during the first 0.5 h (Ga concentration = 110–270 ppm). The asymptotic limit under these test conditions is not clear but testing beyond 4 h provides only a modest reduction of the Ga concentration in PuO_2–Ga_2O_3 powder.

3.3. Effect of sample mass

The effect of sample mass (and thus sample volume) on Ga removal is shown in Fig. 8. It is seen that the quantity of sample processed at one time has no effect on the Ga removal rate or on mass loss for sample sizes of 0.22–25 g. Linear regression of the data supports this conclusion. [2]

3.4. Effect of flow rate

Ga concentration and mass change are plotted as a function of gas flow velocity in Fig. 9 for 2.5 g samples exposed at 1200°C for 4 h. Between 1.5 and 26 cm/s, gas flow rate has no discernible effect on the remaining Ga concentration. In contrast, increasing flow rate increases the mass loss during processing. Linear regression of the data supports the assertion that flow rate affects mass loss but not Ga removal. For 143 observations, it cannot be stated with 95% confidence that flow rate has an effect on the remaining Ga concentration (confidence = 39%). However, for 156 observations, it can be stated with >99.999% confidence that flow rate has an effect on mass change. Similar values are obtained following statistical analysis of DMO material (Ga concentration: 35% confidence, 71 observations; Mass change: >99.995% confidence, 72 observations).

3.5. TIGR from different powders

The Ga concentrations within three-step and DMO powders following processing at 1200°C for 4 h are compared in Fig. 10. The DMO material retained slightly more Ga following exposure for the same duration, even though DMO powder had a smaller starting concentration of Ga. Statistical analysis of the data (student *t*-test, 44 observations) indicates a greater than 99% confidence that the retained Ga concentrations are

[2] Note that linear regression of the data is only a semi-quantitative means for assessing the effects of variables on Ga removal because it is clear that there is no linear relationship between temperature or duration and Ga removal.

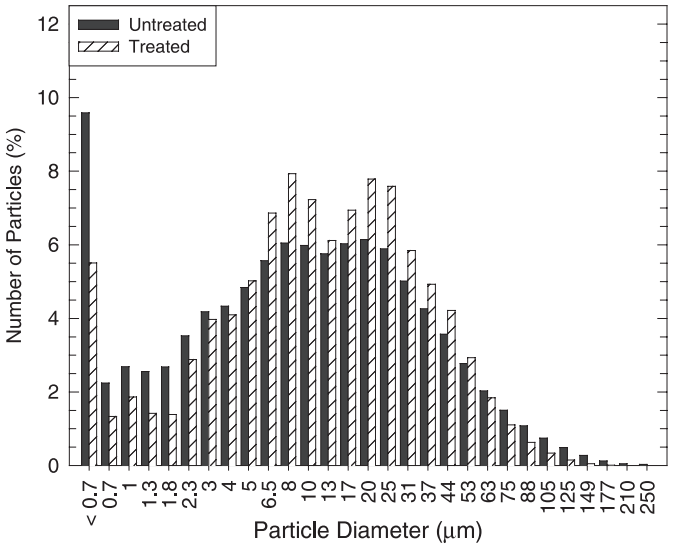

Fig. 5. Three-step powder particle size distribution before and after TIGR (1200°C; 4 h; 1.5 cm/s).

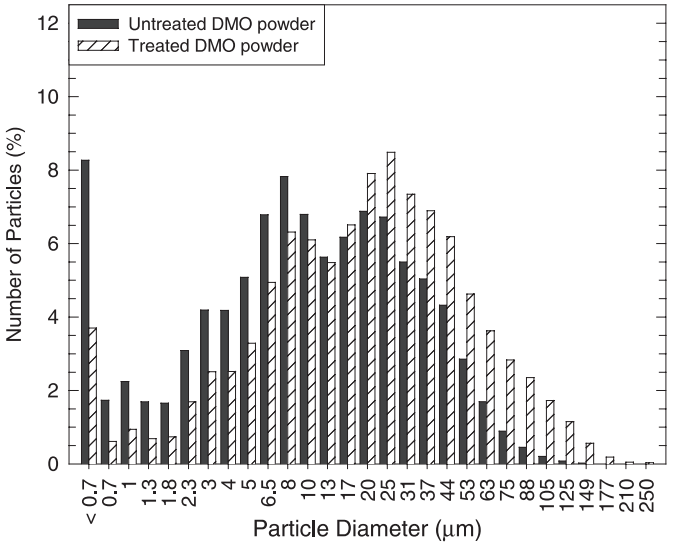

Fig. 6. DMO powder particle size distribution before and after TIGR (1200°C; 4 h; 1.5 cm/s).

different. In contrast to the Ga data, there is a very dramatic difference in the mass changes of the DMO and three-step PuO_2 powders following exposure (Fig. 11). The DMO powder experienced far less mass loss (approximately 1.3%) than the three-step (approximately 2.1%) following a 1200°C exposure for 4 h.

Tests on 2.5 g samples of commercially pure Ga_2O_3 exposed to 900°C or 1200°C Ar–6% H_2 for 4 h were performed. The mass change of the Ga_2O_3 powder far exceeded that of 2.5 g samples of the PuO_2 powders (Fig. 12).

4. Discussion

4.1. Process variable effects

Test duration has an effect on TIGR. The remaining Ga concentration decays roughly exponentially. Thus, increasing exposure time produces diminishing returns. Note that test duration as we define it only incorporates the time at temperature, not the ramp-up and ramp-down time. Therefore, if there is some time–temperature equivalence, the time–temperature integral could be

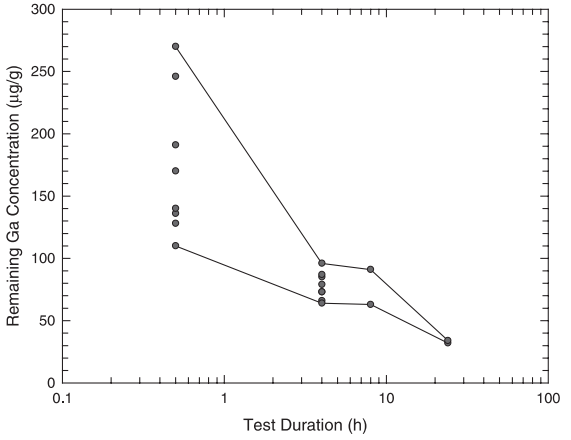

Fig. 7. Remaining Ga concentration in three-step samples as a function of test duration for 0.9 g samples at 1200°C.

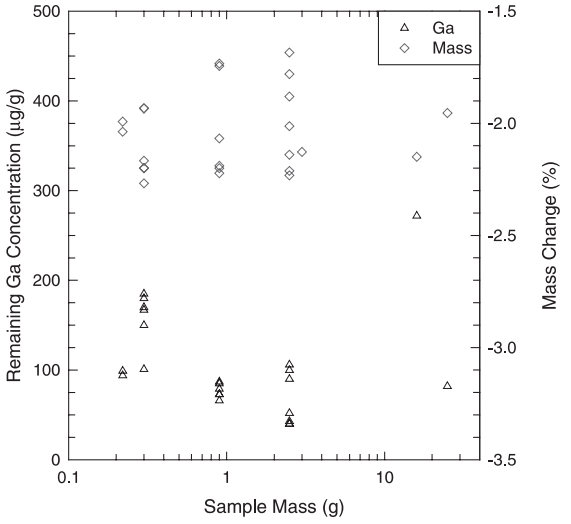

Fig. 8. Remaining Ga concentration and mass change as a function of three-step sample size. Temperature: 1200°C; duration: 4 h; gas flow velocity: 1.5 cm/s.

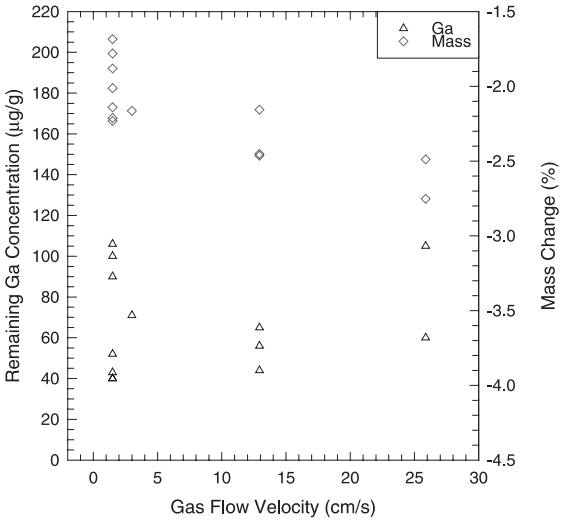

Fig. 9. Remaining Ga concentration in, and mass change of, three-step samples as a function of gas flow velocity. Temperature: 1200°C; duration: 4 h; sample mass: 2.5 g.

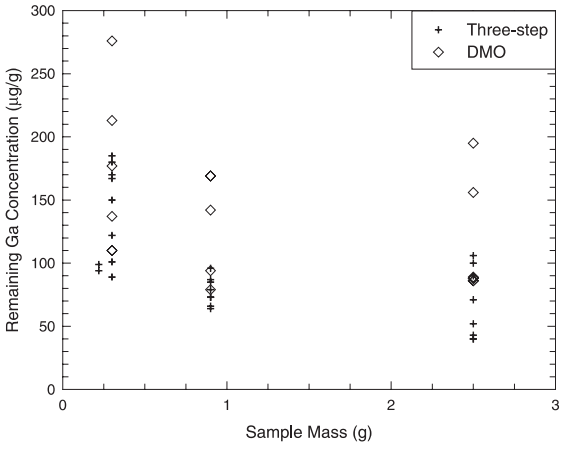

Fig. 10. Comparison of the remaining Ga concentrations within three-step and DMO powders treated at 1200°C for 4 h.

evaluated and added to the test duration to give a more accurate assessment of Ga removal as a function of time. However, given the scatter in the Ga concentration analyses, this refinement of the data may be considered insignificant and, thus, was not performed. Gas flow velocity had an effect on mass change but not on Ga removal. It may be speculated that the primary effect of flow rate on mass loss is attributable to an effect on PuO_2 reduction because Ga evolution and water desorption (LOI) are unaffected by flow rate. Sample volume had no apparent effect on Ga removal for sample masses of 0.2–25 g for the time–temperature combinations in this study.

Of the process variables, temperature plays the strongest role in mass change and Ga removal. Fig. 4 shows that there is significant mass loss between 600°C and 800°C even though there is little Ga evolution at these temperatures. Thus, the majority of the mass loss at the lower temperatures is attributable to something other than Ga evolution, i.e., desorption of water [24] and PuO_2 reduction [25–27]. H_2 gas is a known reductant of PuO_2 [25–27]. At lower temperatures, water desorption dominates mass loss, with essentially all water desorbed at 1000°C [24]. At higher temperatures, a significant fraction of the mass loss is attributable to Ga removal. Some reduction of the PuO_2 occurs above

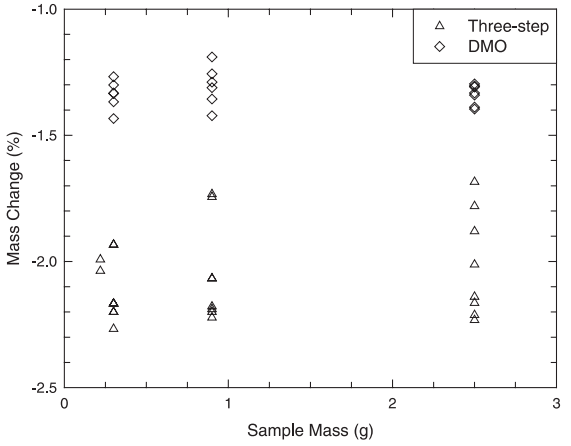

Fig. 11. Comparison of the mass change of three-step and DMO powders treated at 1200°C for 4 h in flowing Ar–6% H_2.

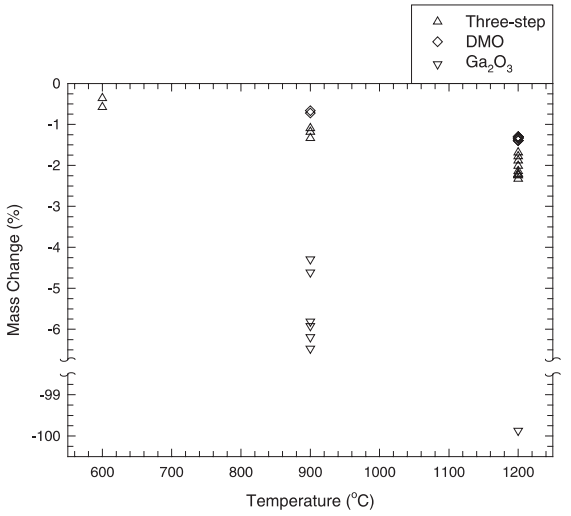

Fig. 12. Plot of mass change as a function of process temperature for different powders exposed to flowing Ar–6% H_2. Test duration: 4 h; Sample mass: 2.5 g; Flow velocity: 1.5 cm/s.

1000°C because full Ga_2O_3 loss (1.12 wt%) and H_2O desorption (0.58 wt%) combined cannot account for the total mass loss of the three-step samples. Mass losses attributable to Ga removal and PuO_2 reduction increase with increasing exposure temperature. A maximum of approximately 4% O_2 loss following PuO_2 reduction is calculated for 1200°C tests.

Regardless of the value of other process parameters, little Ga is removed below 1000°C. Above 1000°C, significant Ga removal occurs during 4 h processing runs. At 1200°C, Ga concentrations as low as 25 ppm were attained (24 h exposure). It is unclear whether there is an ultimate limit for Ga removal or whether the residual

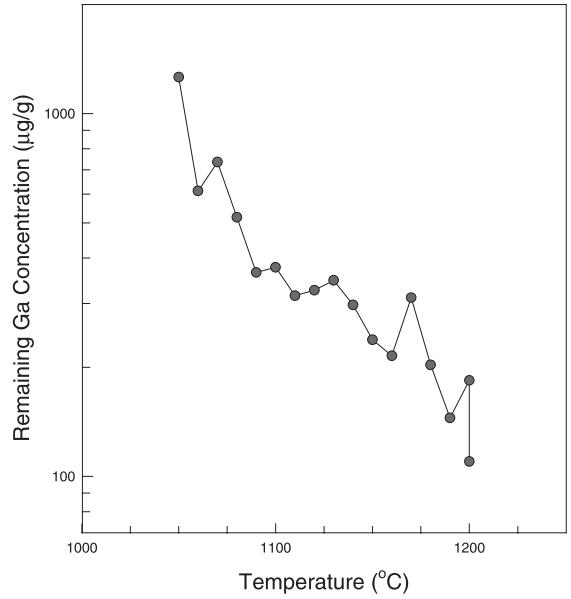

Fig. 13. Plot of remaining Ga concentration as a function of process temperature for 17.5 g DMO samples exposed for 4 h to a 1.5 cm/s gas flow velocity.

Ga concentration can continually be reduced with temperature. Tests employing fine temperature increments between 1050°C and 1200°C suggest that if an ultimate limit exists it is not approached at 1200°C (Fig. 13). Therefore, it is likely that even greater Ga removal could be obtained at higher temperatures.

4.2. Comparison of TIGR from different powders: assessment of the rate limiting step for TIGR

Regardless of the method used to convert Pu–Ga metal to PuO_2–Ga_2O_3 powder, the TIGR process used in this study is effective in separating Ga_2O_3 from PuO_2. The three-step powder experienced greater mass loss due to Ga removal, given its greater starting concentration of Ga and lower final concentration. The DMO material experienced far less mass loss than the three-step powder regardless of process temperature (Fig. 12), sample size (Fig. 11), test duration (not shown), or gas flow velocity (not shown). The difference in mass loss is primarily attributable to reduced water desorption. The starting DMO powder had approximately 0.5 wt% less water adsorbed on its surface as a result of its smaller surface area. Assuming that Ga evolution, water desorption, and PuO_2 reduction are the only mechanisms for mass loss, the amount of reduction can be calculated. The data suggest that the three-step PuO_2 experienced greater reduction by the H_2 gas than the DMO powder, but this cannot be definitively concluded due to the scatter in the data.

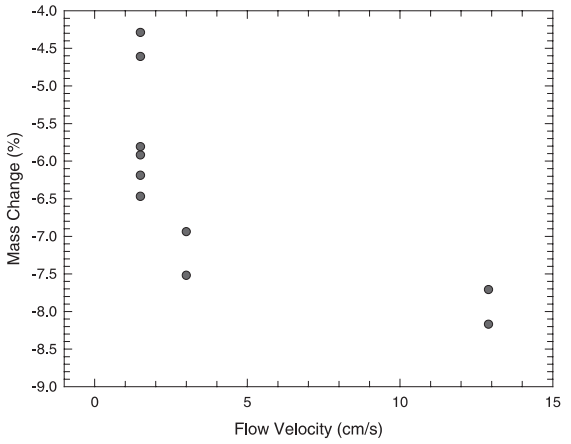

Fig. 14. Plot of mass change as a function of gas flow velocity for 2.5 g samples of commercially pure Ga_2O_3 exposed at 900°C for 4 h.

Ga evolution from commercially pure Ga_2O_3 is much greater than that from either of the Ga_2O_3–PuO_2 powders (Fig. 12). Moreover, for pure Ga_2O_3, increasing gas flow rate increases the rate of Ga evolution (Fig. 14). The increased evolution as compared to PuO_2 and the observed dependence on flow rate indicate that Ga evolution is not reaction rate limited (Eq. (1)) but rather is limited by mass transport. Calculations indicate that in the event of mass transport limitation, Ga_2O will be the limiting species, as opposed to H_2 or H_2O (Fig. 15) [28]. Thus, Ga_2O transport likely limits the Ga_2O evolution from Ga_2O_3. Given that Ga_2O evolution is not reaction rate limited for pure Ga_2O_3, evolution should not be reaction rate limited for PuO_2–Ga_2O_3.

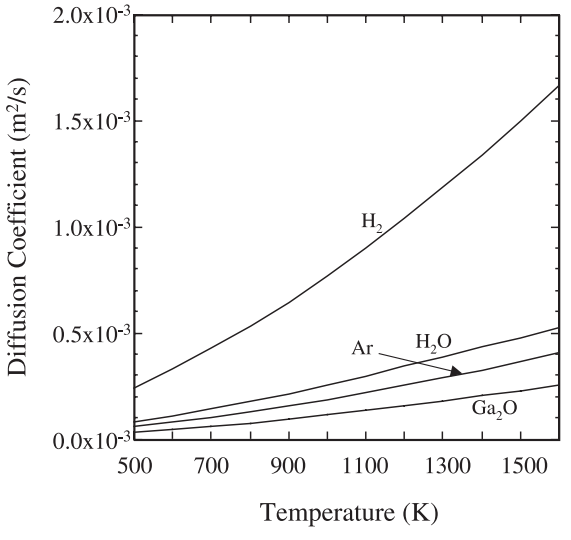

Fig. 15. Diffusion coefficients for relevant gas species as a function of temperature [28].

The fact that Ga removal from PuO_2–Ga_2O_3 powder is unaffected by flow rate suggests that Ga evolution is not limited by mass transport of Ga_2O away from the boat to its deposition point downstream. As Ga evolution does not appear to be either reaction rate limited or mass transport limited by transport away from the boat, the potential rate limiting steps are either mass transport within the PuO_2 particles themselves, or mass transport within the interstices between the powder particles.

The lack of sample volume effect on TIGR suggests that mass transport within the interstices between the powder particles is not rate controlling. 0.3, 0.9 and 2.5 g samples were placed in identical boats. The depth of the powder was approximately 1, 3 and 7 mm for the 0.3, 0.9 and 2.5 g samples. If mass transport within the interstices was rate limiting it would be expected that larger samples would retain more Ga following processing than smaller samples. This was not observed. In order to further assess whether mass transport within the particle interstices controls TIGR, a 0.3 g sample of three-step PuO_2 was spread on an alumina plate so that the powder depth was roughly one tenth of that when in the boat. Enhanced TIGR was not observed for the thinly spread sample. Therefore, although not fully conclusive, it does not appear that mass transport within the powder interstices controls Ga evolution.

Given that the larger DMO particles experience less Ga removal than the smaller three-step particles, it may be hypothesized that TIGR is controlled by mass transport within the powder particles. This hypothesis is supported by the fact that the other mechanisms discussed above do not appear to be controlling. However, it cannot be definitively concluded that the system is under solid-state mass transport control at this time. The experiments performed in this work were designed to determine the optimal processing conditions and were not optimized to determine the controlling mechanisms. Other experiments, such as those incorporating a fluidized bed, would be required to reach a definitive conclusion.

The microstructure of PuO_2–Ga_2O_3 may evolve during processing. Initially, a two-phase microstructure is present because Ga_2O_3 has a low solubility in PuO_2, roughly 45 wppm at 1200°C [23]. Therefore, there is little Ga_2O_3 in solution and the vast majority of the Ga_2O_3 in PuO_2–1 wt% Ga_2O_3 exists as second-phase particles having a Ga_2O_3 activity approaching one. As shown by microprobe measurements of CeO_2 surrogate material [28,29], which is an excellent surrogate for PuO_2 with respect to TIGR [28–30], Ga migrates to grain boundaries during processing in Ar–6% H_2. It has been speculated that the grain boundary compound is not Ga_2O_3 but the perovskite-phase $PuGaO_3$, based on thermodynamic predictions [23,28] and experimental evidence [31]. Note that $PuGaO_3$ is only stable under reducing conditions.

When the Ga concentration is reduced to levels below 45 wppm, it is unclear whether the remaining Ga is primarily in solution in the PuO_2, or whether it is primarily present as a grain boundary compound. The remaining Ga is almost certainly not present as the original second-phase Ga_2O_3 particles because the activity of Ga_2O_3 in these particles is much larger than that in the PuO_2 matrix. Therefore, the driving force for Ga evolution from second-phase particles is much stronger than that from solid solution. It is clear that if there is an ultimate limit for Ga removal, it is below the 45 wppm solubility of Ga_2O_3 in PuO_2, given that 25 wppm Ga remains in PuO_2 following processing at 1200°C for 24 h.

It is clear from the data that the most efficient TIGR from PuO_2 requires the highest temperature achievable, although particle sintering may diminish the benefit from increased temperature under some conditions. In addition to increasing the process temperature, some benefit can be obtained by increasing the exposure duration. However, increasing duration produces diminishing returns. Reducing the starting particle size increases the efficiency of Ga removal, however particle agglomeration during processing (Figs. 5 and 6) limits this benefit. Increasing the intrinsic mass transport at a given temperature would enhance TIGR. However, until the composition and microstructure of Ga within processed powder are better understood, the means for enhancing intrinsic mass transport are unclear. From an industrial standpoint, enhancement of intrinsic mass transport may be preferable to increased temperature, given the increasing attack of furnace materials by Ga_2O with temperature [15].

5. Conclusions

A process for removing Ga_2O_3 from PuO_2 by exposing PuO_2 powder to Ar–6% H_2 gas at elevated temperature was developed. The effects of temperature, exposure duration, gas flow velocity, and sample size on TIGR from different PuO_2 powders were examined. Little Ga removal was observed at process temperatures below 1000°C. Above 1000°C, Ga removal increased with increasing temperature, with as little as 25 ppm remaining in the powder following a 24 h exposure at 1200°C. Processing at 1200°C resulted in both larger particle sizes and reduced surface areas. Increasing test duration increased TIGR, albeit with diminishing returns over time. Limited benefit is obtained by processing beyond 4 h. Gas flow velocity and sample volume did not appear to significantly affect Ga evolution. It is unclear whether there is an ultimate limit for Ga removal, but it appears that TIGR at even greater temperatures could reduce the remaining Ga concentration within PuO_2 even further. Based on TIGR from Ga_2O_3, DMO PuO_2, and three-step PuO_2, it appears that mass transport control within the powder particles limits Ga removal. Further study of the microstructure would be required to determine if the intrinsic mass transport could be enhanced to aid in TIGR.

Acknowledgements

This work was supported by the Office of Fissile Materials Disposition, United States Department of Energy.

References

[1] L.R. Kelman, W.D. Wilkinson, F.L. Yagee, in: Resistance of materials to attack by liquid metals, Argonne National Laboratory Report # ANL-4417, Lemont, IL, 1950.
[2] P.R. Luebbers, W.F. Michaud, O.K. Chopra, Compatibility of ITER candidate structural materials with static gallium, Argonne National Laboratory Report # ANL-93/31, Lemont, IL, December 1993.
[3] M.H. Kamdar, in: ASM Handbook, vol. 11, Failure Analysis and Prevention, American Society for Metals International, Metals Park, OH, 1986, p. 225.
[4] W.D. Wilkinson, Effects of gallium on materials at elevated temperatures, Argonne National Laboratory Report # ANL-5027, Lemont, IL, 1953.
[5] M.H. Kamdar, in: C.L. Briant and S.K. Banerji (Eds.), Treatise on Materials Science and Technology, vol. 25, Academic Press, London, 1983, p. 361.
[6] M.H. Kamdar, Prog. Mater. Sci. 15 (1973) 289.
[7] T.M. Regand, N.S. Stoloff, Metall. Trans. A 8A (1977) 885.
[8] M. Tanaka, H. Fukunaga, J. Soc. Mater. Sci. Jpn. 18 (1969) 411.
[9] B.A. Benson, R.G. Hoagland, Scr. Metall. 23 (1989) 1943.
[10] S.P. Lynch, Acta Metal. 29 (1981) 325.
[11] C.F. Old, P. Trevena, Met. Sci. 13 (1979) 591.
[12] J.A. Kargol, D.L. Albright, Metall. Trans. A 8A (1977) 27.
[13] J.T. Lukowski, D.B. Kasul, L.A. Heldt, C.L. White, Scr. Metall. 24 (1990) 1959.
[14] D.G. Kolman, Corros. Sci. 42 (2000) in press.
[15] D.G. Kolman, T.N. Taylor, Y.S. Park, M. Stan, D.P. Butt, C.J. Maggiore, J.R. Tesmer, G.J. Havrilla, Gallium Suboxide Attack of Stainless Steel and Nickel Alloys at 800°C–1200°C, Los Alamos National Laboratory Report # LA-UR-00-0864, February 2000; submitted to Oxidation of Metals.
[16] D.F. Wilson, J.R. DiStefano, J.P. Strizak, J.F. King, E.T. Manneschmidt, Interactions of zircaloy cladding with gallium: Final Report, Oak Ridge National Laboratory Technical Report No. ORNLTM-13684, Oak Ridge, TN, September 1998.
[17] P.H. Au-Yeung, J.T. Lukowski, L.A. Heldt, C.L. White, Scr. Metall. 24 (1990) 95.
[18] M.K. West, Gallium interactions with zircaloy, Amarillo National Resource Center for Plutonium Technical Report No. ANRCP-1999-2, Amarillo, TX, January 1999.

[19] R.R. Hart, J. Rennie, K. Aucoin, M. West, K. Ünl and C. Ríos-Martinez, Gallium Interactions with Zircaloy Cladding, Amarillo National Resource Center for Plutonium Report ANRCP-1998-5, Amarillo, TX, 1998.
[20] J.M. Cleveland, in: O.J. Wick (Ed.), Plutonium Handbook, A guide to the Technology, vol. 1, American Nuclear Society, La Grange Park, IL, 1980, p. 553.
[21] T.M. Besmann, J. Am. Ceram. Soc. 81 (1998) 3071.
[22] D.P. Butt, Y. Park, T.N. Taylor, J Nucl Mater 264 (1999) 71.
[23] H.R. Trellue, T. Baros, H.T. Blair, J.J. Buksa, D.P. Butt, K. Chidester, S.F. De Muth, S.L. Eaton, R. Hanrahan, G.J. Havrilla, C.A. James, D.G. Kolman, R.E. Mason, Y. Park, M. Stan, J.H. Steele Jr., S.S. Voss, T.C. Wallace Sr., C.G. Worley, Nuclear Fuels Technologies Fiscal Year 1997 Research and Development Test Results, Los Alamos National Laboratory Report # LA-UR-97-4423, Los Alamos, NM, October 1997.
[24] J.L. Stakebake, L.M. Steward, J. Colloid Interf. Sci. 42 (1973) 328.
[25] E.R. Gardner, T.L. Markin, R.S. Street, J. Inorg. Nucl. Chem. 27 (1965) 541.
[26] H.E. Flotow, M. Tetenbaum, J. Chem. Phys. 74 (1981) 5269.
[27] R.L Deaton, G.L. Silver, Radiochem. Radioanal. Lett. 10 (1972) 277.
[28] H.R Trellue, D.P. Butt, S.F De Muth, S.L. Eaton, R. Hanrahan, G.J. Havrilla, C. Haertling, C.A. James, D.G. Kolman, R.E. Mason, P. Chodak, A.D. Neuman, Y. Park, C.A. Smith, M. Stan, S.A. Talachy, J. Teague, C.G. Worley, Nuclear Fuels Technologies Fiscal Year 1998 Research and Development; Summary of Test Results, Los Alamos National Laboratory Report # LA-UR-98-5355, Los Alamos, NM, November 1998.
[29] Y. Park, D.G. Kolman, H. Ziraffe, C. Haertling, D.P. Butt, Mater. Res. Soc. Symp. Proc. 556 (1999) 129.
[30] D.G. Kolman, Y. Park, M. Stan, R.J. Hanrahan Jr., D.P. Butt, An assessment of the validity of cerium oxide as a surrogate for plutonium oxide gallium removal studies, Los Alamos National Laboratory Report # LA-UR-99-491, Los Alamos, NM, January 1999.
[31] J.R. Schoonover, A. Saab, J.S. Bridgewater, G.J. Havrilla, C.T. Zugates, P.J. Treado, Appl. Spectrosc. 54 (2000) in press.